Quadratic Program based Nonlinear Embedded Control of Series Elastic Actuators

Aaron D. Ames and James Holley

***Abstract*— This paper presents a method for embedded motor control based upon rapidly exponentially stabilizing control Lyapunov functions (RES-CLFs) implemented through Quadratic Programs (QPs). This will give guaranteed exponential convergence via an optimal nonsmooth nonlinear embedded level controller that provides the minimal control effort necessary to achieve the desired convergence in torque. Utilizing this novel control methodology, we are able to formally establish that the dynamics of series elastic systems can be approximated by rigid system models. Importantly, the RES-CLF based QP is presented in a way that will allow for its real-time implementation at the embedded level via a closed form solution to a QP; the end result is a nonlinear optimal controller able to run at over 5kHz. To demonstrate this, simulation and experimental results are presented showing the performance of the embedded controller.**

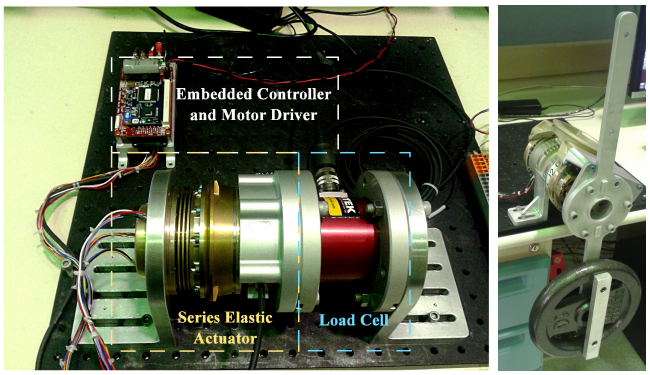

Fig. 1. Experimental setup used to test embedded RES-CLF based QPs: (left) locked output case (right) free output case used for disturbance testing.

I. Introduction

Series elastic actuators (SEAs) have the potential to provide a powerful means for which to achieve torque control on robotic systems [9], [13], [14], especially in the context of robotic locomotion [12], [15], [20]. The general premise of SEAs is that adding a spring between the motor and joint allows for torque to be measured. Through this measurement, embedded level controllers can be utilized to track desired torques being communicated from a controller operating with only knowledge of the rigid dynamics of the robot. Thus, the ultimate goal is to decouple the actuator dynamics of the robot from the rigid body dynamics for the purposes of pure torque control. Yet this objective is often fraught with practical issues; namely, robotic systems with SEAs have higher order dynamics due to the presence of the springs—these dynamics, even through the use of embedded controllers, cannot be completely decoupled from the idealized rigid body dynamics for which controllers are designed. The end result is often either instability or the "detuning" of embedded level controllers that ultimately prevents the pure application of torque controllers and, thereby, eliminates the benefits of SEAs.

As a means to mathematically formulate the goals of SEAs in robotic systems, the main contribution of this paper is a novel embedded controller that formally allows for the rigid body dynamics and the motor dynamics to be decoupled. This provides further theoretic foundation for achieving the benefits of SEAs, especially with regard to torque control, while ideally circumventing their shortcomings.

Motivated by the classical work of Spong [19] and the time-scale separation of singularly perturbed systems [11], we apply the framework of rapidly exponentially stabilizing control Lyapnov functions (RES-CLFs) [2], [3], at the embedded level, to achieve time-scale separation between the actuator and rigid body dynamics of the robot. RES-CLFs have proven effective in the control of robotic systems in the context of bipedal locomotion [3], [8] due to the fact that they guarantee exponential convergence at a desired rate of $\frac{1}{\varepsilon} > 0$, i.e.,

$$\varepsilon \dot{V}(x,u) \leq -\gamma V(x)$$

for a RES-CLF V and the proper choice of control input u. With the observation that ε can be viewed as a time-scaling factor, $\tau = \frac{t}{\varepsilon}$, the existence of a RES-CLF suggests the ability to create dynamics operating at different time-scales. Therefore, applying RES-CLFs to the actuator dynamics in a series elastic robotic system allows for the separation of the actuator dynamics from the rigid body dynamics.

To formally establish the decoupling afforded by RES-CLFs, we begin by formulating properties of a specific class of RES-CLFs applied to rigid body robotic systems (Sect. III) after introducing the based definitions needed (Sect. II). These RES-CLFs are then applied to the model of a series elastic actuator isolated from the rigid body dynamics of the system in Sect. IV; in particular, the RES-CLF naturally yields a quadratic program (QP) that minimizes actuator torque while achieving a desired convergence rate. Implementing this QP through its closed form solution yields a nonlinear nonsmooth embedded controller. We return to the

Aaron D. Ames is with the Department of Mechanical Engineering and the Department of Electrical & Computer Engineering, and James Holley is with the Department of Electrical & Computer Engineering, Texas A&M University, College Station, TX 77843. *aames@tamu.edu*; The research of Aaron D. Ames is supported by NASA NNX11AN06H, NASA NNX12AQ68G, NSF CNS-0953823, NSF CNS-1136104.

full-order SEA model in Sect. V and, through the separation of time scales afforded by the RES-CLF based embedded controller, we establish the main result of this paper: the dynamics of the full-order SEA model can be effectively decoupled into a rigid body system and isolated motor dynamics. In particular, by considering outputs in the joint coordinates and a RES-CLF controller for the rigid body dynamics that drives these outputs to zero exponentially, we prove that the outputs display the same convergence up to $O(\varepsilon)$ for the full-order SEA model with the RES-CLF embedded motor controller.

To demonstrate the results of the paper, we focus on evaluating the RES-CLF embedded controller—and its QP based representation—both in simulation and experimentally (Sect. VI). In particular, the controller is experimentally evaluated on a series elastic actuator with a fixed output (see Fig. 1). The performance of the controller is tested in the context of tracking a variety of time-based torque signals for which accurate tracking is observed. Finally, as a means to approximate the embedded controller performance in the context of (unknown) rigid body dynamics, external disturbances are applied to the joint. Ultimately, the embedded RES-CLF based QP controller performs well experimentally.

II. Rapidly Exponentially Stabilizing Control Lyapunov Functions

We begin by giving a brief overview of rapidly exponentially stabilizing control Lyapunov functions (CLFs) in the context of nonlinear systems, which extend classical notions of CLFs [5], [17], [18] in order to achieve "rapid" exponential convergence.

Consider an nonlinear affine control systems of the form

$$\begin{aligned} \dot{x} &= f(x,z) + g(x,z)u \\ \dot{z} &= q(x,z), \end{aligned} \tag{1}$$

where $x \in X$ are controlled (or output) states, $z \in Z$ are the uncontrolled states, and U is the set of admissible control values for u. In addition, we assume that $f(0,z) = 0$, i.e., that the zero dynamics surface Z defined by $x = 0$ with dynamics given by $\dot{z} = q(0,z)$ is invariant.

In this paper, we will focus on two forms of control Lyapunov functions: *exponentially stabilizing* and *rapidly exponentially stabilizing*. The interplay between these two types of CLFs will become clear in the context of time-scaling as discussed in Sect. V.

Definition 1: *A continuously differentiable function $V : X \to \mathbb{R}$ is an* **exponentially stabilizing control Lyapunov function (ES-CLF)** *if there exist positive constants $c_1, c_2, c_3 > 0$ such that*

$$c_1\|x\|^2 \leq V(x) \leq c_2\|x\|^2 \tag{2}$$

$$\inf_{u \in U} \left[L_f V(x,z) + L_g V(x,z)u + c_3 V(x)\right] \leq 0 \tag{3}$$

for all $(x,z) \in X \times Z$.

Motivated by the desire to achieve rapid exponential convergence we introduce the following augmented definition.

Definition 2: *A continuously differentiable function $V_\varepsilon : X \to \mathbb{R}$ is a* **rapidly exponentially stabilizing control Lyapunov function (RES-CLF)** *[2], [3] if there exist positive constants $c_1, c_2, c_3 > 0$ such that for all $0 < \varepsilon < 1$*

$$c_1\|x\|^2 \leq V_\varepsilon(x) \leq \frac{1}{\varepsilon^2} c_2\|x\|^2 \tag{4}$$

$$\inf_{u \in U} \left[L_f V_\varepsilon(x,z) + L_g V_\varepsilon(x,z)u + \frac{1}{\varepsilon} c_3 V_\varepsilon(x)\right] \leq 0 \tag{5}$$

for all $(x,z) \in X \times Z$.

Min-Norm Controller. The existence of a RES-CLF yields a family of controllers that rapidly exponentially stabilize the system to the zero dynamics [6], [18]. In particular, we can consider the control values:

$$\begin{aligned} K_\varepsilon(x,z) = & \\ & \{u \in U : L_f V_\varepsilon(x,z) + L_g V_\varepsilon(x,z)u + \frac{1}{\varepsilon} c_3 V_\varepsilon(x) \leq 0\}, \end{aligned} \tag{6}$$

where L is the Lie derivative [16]. It follows that:

$$\begin{aligned} u_\varepsilon(x,z) \in K_\varepsilon(x,z) \qquad & \Rightarrow \\ \|x(t)\| \leq \frac{1}{\varepsilon}\sqrt{\frac{c_2}{c_1}} e^{-\frac{1}{\varepsilon}\frac{c_3}{2}t}\|x(0)\|. & \end{aligned} \tag{7}$$

In addition, this yields specific feedback controllers, e.g., the min-norm controller:

$$\begin{aligned} m_\varepsilon(x,z) &= \operatorname{argmin}\{\|u\| : u \in K_\varepsilon(x,z)\} \\ &= \operatorname{argmin}\{\|u\| : \psi_{0,\varepsilon}(x) + \psi_{1,\varepsilon}^T(x)u \leq 0\} \end{aligned}$$

where

$$\begin{aligned} \psi_{0,\varepsilon}(x,z) &= L_f V_\varepsilon(x,z) + \frac{1}{\varepsilon}\gamma V_\varepsilon(x,z) \\ \psi_{1,\varepsilon}(x,z) &= L_g V_\varepsilon(x,z)^T \end{aligned} \tag{8}$$

While controller $m(x,z)$ that minimizes the control effort u can be stated in closed form as:

$$m(x,z) = \begin{cases} -\frac{\psi_{0,\varepsilon}(x,z)\psi_{1,\varepsilon}(x,z)}{\psi_{1,\varepsilon}(x,z)^T\psi_{1,\varepsilon}(x,z)} & \text{if} \quad \psi_{0,\varepsilon}(x,z) > 0 \\ 0 & \text{if} \quad \psi_{0,\varepsilon}(x,z) \leq 0 \end{cases}$$

it is important to note that this closed form solution is the solution to the quadratic program (QP):

$$\begin{aligned} m(x,z) = \underset{u \in U}{\operatorname{argmin}} \quad & u^T u \\ \text{s.t.} \quad & \psi_{0,\varepsilon}(x,z) + \psi_{1,\varepsilon}^T(x,z)u \leq 0 \quad \text{(CLF)} \end{aligned} \tag{9}$$

This formulation leads to a new class of controllers based upon CLF based QPs; these have been applied to locomotion and manipulation in bipedal robots [4], and have been utilized to experimentally achieve robotic walking [7], [8].

III. RES-CLF Constructions

This section considers rigid body dynamics for a robotic system and, based upon the desire to drive an output function $y \to 0$, constructs a specific class of RES-CLFs. Importantly, a majority of this section is devoted to establishing the properties of this class of RES-CLFs. Of particular note is the relationship between RES-CLFs and ES-CLFs that can be established through the use of time-scaling.

Robotic Systems. Let Q be the configuration space of a robot with n degrees of freedom, i.e., $n = \dim(Q)$, with coordinates $q \in Q$. For the sake of definiteness, it may be necessary to choose Q to be a subset of the actual configuration space of the robot so that global coordinates can be defined[1], i.e., such that Q is embeddable in $\mathbb{R}^n$, or more simply $Q \subset \mathbb{R}^n$. Consider the equations of motion for a robot given in the general form by the Euler-Lagrange equations:

$$M(q)\ddot{q} + H(q, \dot{q}) = u, \tag{10}$$

where M is the inertia matrix, H is a vector containing the coriolis and gravity terms. Here, for the sake of simplicity, we assume full actuation and thus consider control inputs $u \in \mathbb{R}^n$. We also assume, as in [19], that the inertia matrix $M(q)$ is symmetric, positive definite, and both $M(q)$ and $M(q)^{-1}$ are uniformly bounded as functions of $q \in \mathbb{R}^n$.

Output Dynamics. Consider an output function $y : Q \to \mathbb{R}^n$, and the control objective of driving $y(q) \to 0$ exponentially. Differentiating y twice yields the output dynamics:

$$\ddot{y}(q) = D_y(q)\ddot{q} + \dot{D}_y(q, \dot{q})\dot{q} \tag{11}$$

where $D_y(q) = \frac{\partial y}{\partial q}(q)$ is the Jacobian of the output y. Substituting in the dynamics of the robotic system (10) yields:

$$\ddot{y} = \underbrace{-D_y M^{-1} H + \dot{D}_y \dot{q}}_{L_f^2(q,\dot{q})} + \underbrace{D_y M^{-1}}_{A(q,\dot{q})} u, \tag{12}$$

where the dependence on q and $\dot{q}$ was removed for notational simplicity. Letting $x = (y, \dot{y})$, then (12) can be written in the general form of (1) as follows:

$$\dot{x} = \underbrace{\begin{bmatrix} x_2 \\ L_f^2(x) \end{bmatrix}}_{f(x)} + \underbrace{\begin{bmatrix} 0 \\ A(x) \end{bmatrix}}_{g(x)} u \tag{13}$$

where L_f^2 and A can be expressed in terms of the coordinates x due to the standard diffeomorphism [16]. Also note that, in this case, since we are assuming full-actuation the zero dynamics in (1) do not exist, leaving only the output dynamics.

Assume that the decoupling matrix, A, is invertible, i.e., that y has (vector) relative degree 2, we can choose the control law:

$$u = A^{-1}(-L_f^2 + \mu) = M D_y^{-1}(\mu - \dot{D}_y \dot{q}) + H \tag{14}$$

for some $\mu \in \mathbb{R}^n$ resulting in

$$\ddot{y} = \mu. \tag{15}$$

This choice of control law allows us to write the output dynamics (13) as:

$$\dot{x} = \underbrace{\begin{bmatrix} 0 & I \\ 0 & 0 \end{bmatrix}}_{F} x + \underbrace{\begin{bmatrix} 0 \\ I \end{bmatrix}}_{G} \mu \tag{16}$$

[1]Note that at various points we will assume that matrix functions have full rank; it may be necessary to carefully choose Q to satisfy these conditions.

RES-CLF Construction. With the error dynamics in hand, in order to construct a RES-CLF, we first consider the continuous time algebraic Riccati equations (CARE):

$$F^T P + PF - PGG^T P + Q = 0 \tag{17}$$

for any $Q = Q^T > 0$ and with solution $P = P^T > 0$. One can use P to construct a RES-CLF that will stabilize the dynamics at a user defined rate of $\frac{1}{\varepsilon}$. In particular, define

$$V_\varepsilon(x) = x^T \underbrace{I_\varepsilon P I_\varepsilon}_{P_\varepsilon} x, \qquad \text{with} \quad I_\varepsilon = \operatorname{diag}(\frac{1}{\varepsilon} I, I), \tag{18}$$

wherein it follows that:

$$\dot{V}_\varepsilon(x) = L_F V_\varepsilon(x) + L_G V_\varepsilon(x)\mu$$

with

$$\begin{aligned} L_F V_\varepsilon(x) &= x^T(F^T P_\varepsilon + P_\varepsilon F)x \\ L_G V_\varepsilon(x) &= 2x^T P_\varepsilon G \end{aligned} \tag{19}$$

It follows that, in this case, (6) takes the form:

$$K_\varepsilon(x) = \{\mu \in \mathbb{R}^n : L_F V_\varepsilon(x) + L_G V_\varepsilon(x)\mu + \frac{1}{\varepsilon}\gamma V_\varepsilon(x) \le 0\}. \tag{20}$$

Note that it is easy to verify that, for the dynamics given in (34) and for P_ε defined in (18), $V(x) = x^T P_\varepsilon x$ is a RES-CLF with

$$c_1 = \lambda_{\min}(P), \quad c_2 = \lambda_{\max}(P), \quad c_3 = \gamma = \frac{\lambda_{\min}(Q)}{\lambda_{\max}(P)}. \tag{21}$$

This can be seen by noting that, from (17) and the form of F and G that P_ε solves the RES-CARE:

$$F^T P_\varepsilon + P_\varepsilon F - \frac{1}{\varepsilon} P_\varepsilon G G^T P_\varepsilon + \frac{1}{\varepsilon} I_\varepsilon Q I_\varepsilon = 0, \tag{22}$$

noting that $\gamma P_\varepsilon \le I_\varepsilon Q I_\varepsilon$ and therefore

$$\begin{aligned} &\inf_\mu \left[L_F V_\varepsilon(x) + L_G V_\varepsilon(x)\mu + \frac{1}{\varepsilon}\gamma V_\varepsilon(x) \right] \\ &\quad \le \inf_\mu \left[x^T P_\varepsilon G (\frac{1}{\varepsilon} G^T P_\varepsilon x + 2\mu) \right] \le 0 \end{aligned} \tag{23}$$

which can be seen by noting that for $\mu = -\frac{1}{2\varepsilon} G^T P_\varepsilon x$

$$x^T P_\varepsilon G (\frac{1}{\varepsilon} G^T P_\varepsilon x + 2\mu) = 0.$$

These facts allow us to establish the following specific bounds on the convergence of y:

Lemma 1: *For the output dynamics given by* (13) *and the RES-CLF $V_\varepsilon(x) = x^T P_\varepsilon x$, with P_ε a solution to the RES-CARE* (22)*, for any control law*

$$u_\varepsilon(x) = A(x)^{-1}(-L_f^2(x) + \mu_\varepsilon(x))$$

with $\mu_\varepsilon(x) \in K_\varepsilon(x)$ Lipschitz continuous, it follows that:

$$\left\| \begin{matrix} y(t) \\ \dot{y}(t) \end{matrix} \right\| \le \frac{1}{\varepsilon} \sqrt{\frac{\lambda_{\max}(P)}{\lambda_{\min}(P)}} e^{-\frac{1}{\varepsilon}\frac{\lambda_{\min}(Q)}{2\lambda_{\max}(P)} t} \left\| \begin{matrix} y(0) \\ \dot{y}(0) \end{matrix} \right\|$$

Thus the output dynamics are exponentially stable at the origin.

Relationship with Time-Scaling. The original development of RES-CLFs was motivated by time-scaling based upon ε [2]. We will revist this original motivation in the context of RES-CLFs to establish their relationship with ES-CLFs.

For $\mu_\varepsilon(x) \in K_\varepsilon(x)$, since V_ε is a RES-CLF it implies that

$$\varepsilon \dot{V}_\varepsilon(x, \mu_\varepsilon(x)) \leq -\gamma V_\varepsilon(x).$$

Therefore, choosing the time-scaling $\tau = \frac{1}{\varepsilon} t$ we have

$$\frac{d}{d\tau} V_\varepsilon(x(\tau), \mu_\varepsilon(x(\tau))) \leq -\gamma V_\varepsilon(x(\tau)).$$

Defining the state variables:

$$x_\varepsilon := I_\varepsilon x = \begin{bmatrix} \frac{1}{\varepsilon} y \\ \dot{y} \end{bmatrix} \tag{24}$$

it follows that

$$V_\varepsilon(x) = x_\varepsilon^T P x_\varepsilon =: V(x_\varepsilon) \tag{25}$$

with P the solution to the CARE (17). As a result, it is easy to verify that

$$\frac{d}{d\tau} V(x_\varepsilon(\tau), \varepsilon \mu_\varepsilon(x(\tau))) \leq -\gamma V(x_\varepsilon(\tau)). \tag{26}$$

where, again, $\mu_\varepsilon(x(\tau)) \in K_\varepsilon(x(\tau))$.

This allows us to establish the time-scaling property for the class of RES-CLFs being considered:

Proposition 1: *$V_\varepsilon(x) = x^T P_\varepsilon x$ is a RES-CLF for the control system* (34) *if and only if $V(x_\varepsilon) = x_\varepsilon^T P x_\varepsilon$ is a ES-CLF for the system:*

$$\varepsilon \dot{x}_\varepsilon = F x_\varepsilon + G \varepsilon \mu \tag{27}$$

Moreover,

$$\begin{aligned} \mu \in \overline{K}_\varepsilon(x) \quad &:= \{\mu \in \mathbb{R}^n : x^T P_\varepsilon G(\frac{1}{\varepsilon} G^T P_\varepsilon x + 2\mu) \leq 0\} \\ \Updownarrow & \\ \varepsilon\mu \in \overline{K}(x_\varepsilon) \quad &:= \{\mu \in \mathbb{R}^n : x_\varepsilon^T P G(G^T P x_\varepsilon + 2\mu) \leq 0\}. \end{aligned} \tag{28}$$

Before proving this result we note that the motivation for considering the set $\overline{K}_\varepsilon(x)$ is that, by (23),

$$\overline{K}_\varepsilon(x) \subset K_\varepsilon(x).$$

Therefore, control values in $\overline{K}_\varepsilon(x)$ will still rapidly exponentially stabilize the system (34).

Proof: We begin by noting that, from (23), it follows that

$$\overline{K}_\varepsilon(x) \subset K_\varepsilon(x).$$

To establish this result, note that system given in (27) is obtained by applying the coordinate transformation $x \mapsto I_\varepsilon x$. With the time-scaling $\tau = \frac{1}{\varepsilon} t$, it follows from (27) that

$$\frac{dx_\varepsilon}{d\tau} = F x_\varepsilon + G \varepsilon \mu. \tag{29}$$

Therefore, by the inequality (23), the result follows from (25) and (26) if (28) holds. In particular, the conditions in Def. 1 will be satisfied with the same values for c_1, c_2 and c_3 stated in (21).

The relationship given in (28) is easily established by noting that, due to the special form of G being considered (34) it follows that $I_\varepsilon G = G$ and $I_\varepsilon^T = I_\varepsilon$. Therefore,

$$\begin{aligned} & x^T P_\varepsilon G(\frac{1}{\varepsilon} G^T P_\varepsilon x + 2\mu) \leq 0 \\ \Leftrightarrow \quad & x^T P_\varepsilon G(G^T P_\varepsilon x + 2\varepsilon\mu) \leq 0 \\ \Leftrightarrow \quad & x^T I_\varepsilon P I_\varepsilon G(G^T I_\varepsilon P I_\varepsilon x + 2\varepsilon\mu) \leq 0 \\ \Leftrightarrow \quad & x_\varepsilon^T P G(G^T P x_\varepsilon + 2\varepsilon\mu) \leq 0 \end{aligned}$$

as desired. ■

IV. Motor Dynamics & Control

Consider a single series elastic actuator with dynamics:

$$J\ddot{\theta}_\Delta + b\dot{\theta}_\Delta + k\theta_\Delta = \tau_m \tag{30}$$

Given a desired torque as delivered from a "high-level" control value, τ_d (assumed to be constant in this section), the goal is to drive the measured torque:

$$\tau_s = k\theta_\Delta$$

obtained from the spring to the desired torque. In other words, the control objective is:

$$\text{Drive} \quad e := k\theta_\Delta - \tau_d \to 0 \quad \text{exponentially.} \tag{31}$$

We will achieve this convergence, in a torque optimal fashion at a desired exponential rate, with a RES-CLF based QP.

Error Dynamics. With the control objective in hand, we can write the error dynamics as:

$$\frac{J}{k}\ddot{e} + \frac{b}{k}\dot{e} + e + \tau_d = \tau_m \tag{32}$$

where $\dot{e} = k\dot{\theta}_\Delta$ and $\ddot{e} = k\ddot{\theta}_\Delta$. Picking the feedback control law:

$$\tau_m = \frac{J}{k}\mu + \frac{b}{k}\dot{e} + e + \tau_d \tag{33}$$

for a secondary controller, μ, implies that

$$\ddot{e} = \mu$$

Now, the goal is to design the controller μ that will drive the error to zero. In particular, we note that, in this case, we can write the error dynamics, with $z = (e, \dot{e})^T \in \mathbb{R}^2$, as

$$\dot{z} = \underbrace{\begin{bmatrix} 0 & 1 \\ 0 & 0 \end{bmatrix}}_{F_m} x + \underbrace{\begin{bmatrix} 0 \\ 1 \end{bmatrix}}_{G_m} \mu \tag{34}$$

Control Law Construction. Utilizing the RES-CLF $V_\varepsilon(z) = z^T P_\varepsilon z$, we can convert this RES-CLF back to both the coordinates of the original system, θ_Δ and $\dot{\theta}_\Delta$, along with converting μ back to a control law in τ_m.

Since the error coordinates, $z = (e, \dot{e})^T$, are functions of θ_Δ, τ_d and $\dot{\theta}_\Delta$ the CLF conditions become:

$$\psi_{0,\varepsilon}(\theta_\Delta, \dot{\theta}_\Delta, \tau_d) + \psi_{1,\varepsilon}^T(\theta_\Delta, \dot{\theta}_\Delta, \tau_d)\mu \leq 0$$

$$m(\theta_\Delta, \dot\theta_\Delta, \tau_d) = \underset{\tau_m \in \mathbb{R}}{\operatorname{argmin}} \quad \tau_m^2 \qquad \text{(Motor QP)}$$

$$\text{s.t.} \quad \psi_{0,\varepsilon}(\theta_\Delta, \dot\theta_\Delta, \tau_d) + \frac{k}{J}\psi_{1,\varepsilon}^T(\theta_\Delta, \dot\theta_\Delta, \tau_d)\left(\tau_m - b\dot\theta_\Delta - k\theta_\Delta\right) \le 0 \qquad \text{(CLF Constraint)}$$

for $\psi_{0,\varepsilon}$ and $\psi_{1,\varepsilon}$ as defined in (8) with $L_{F_m}V_\varepsilon(\theta_\Delta, \dot\theta_\Delta)$ and $L_{G_m}V_\varepsilon(\theta_\Delta, \dot\theta_\Delta)$ given in (19). Finally, we can convert this inequality back to an inequality in τ_m by noting that:

$$\mu = \frac{k}{J}\left(\tau_m - b\dot\theta_\Delta - k\theta_\Delta\right)$$

Therefore, the final form of the CLF constraint, as a function of the original variables, is:

$$\psi_{0,\varepsilon}(\theta_\Delta, \dot\theta_\Delta, \tau_d) + \psi_{1,\varepsilon}^T(\theta_\Delta, \dot\theta_\Delta, \tau_d)\frac{k}{J}\left(\tau_m - b\dot\theta_\Delta - k\theta_\Delta\right) \le 0$$

With this constraint, we can consider the min-norm controller, expressed as a QP as given in (Motor QP). Finally, we can express this controller in closed form by defining:

$$\begin{aligned}\overline{\psi}_{0,\varepsilon}(\theta_\Delta, \dot\theta_\Delta, \tau_d) &= \psi_{0,\varepsilon}(\theta_\Delta, \dot\theta_\Delta, \tau_d) \\ &\quad -\frac{k}{J}\psi_{1,\varepsilon}^T(\theta_\Delta, \dot\theta_\Delta, \tau_d)\left(b\dot\theta_\Delta + k\theta_\Delta\right) \\ \overline{\psi}_{1,\varepsilon}(\theta_\Delta, \dot\theta_\Delta, \tau_d) &= \frac{k}{J}\psi_{1,\varepsilon}^T(\theta_\Delta, \dot\theta_\Delta, \tau_d)\end{aligned} \tag{35}$$

wherein it follows that:

$$m(z) = \begin{cases} -\frac{\overline{\psi}_{0,\varepsilon}(z)\overline{\psi}_{1,\varepsilon}(z)}{\overline{\psi}_{1,\varepsilon}(z)^T\overline{\psi}_{1,\varepsilon}(z)} & \text{if} \quad \overline{\psi}_{0,\varepsilon}(z) > 0 \\ 0 & \text{if} \quad \overline{\psi}_{0,\varepsilon}(z) \le 0 \end{cases} \tag{36}$$

V. Robotic Systems with Series Elastic Actuators

Utilizing the methods developed thus far, we present the main result of this paper: the dynamics of the full-order SEA model can be effectively decoupled into a rigid body system and isolated motor dynamics. This is achieved through the time-scale separation implied by the results of Sect. III, and the observation that the scaling afforded by ε is naturally amenable to singular perturbation theory.

SEA System Model. We begin by presenting the model for a robotic system with series elastic actuators [12], [19]. In particular, we assume dynamics of the form:

$$M(q)\ddot q + H(q, \dot q) = k(q_m - q) + b(\dot q_m - \dot q), \tag{37}$$

$$J\ddot q_m + b(\dot q_m - \dot q) + k(q_m - q) = u_m \tag{38}$$

where q is the joint angle, q_m is the motor angle, u_m torque input to the motor, $k \in \mathbb{R}^{n\times n}$ is a diagonal matrix of spring constants for each series elastic actuator, $b \in \mathbb{R}^{n\times n}$ is a diagonal matrix of damping constants for each SEA, and $J \in \mathbb{R}^{n\times n}$ is a diagonal matrix of motor inertias. Note that, since k and b are diagonal matrices, we will write their inverse by "$\frac{1}{k}$" and "$\frac{1}{b}$," respectively, so as to denote the component-wise inverse of the diagonal elements.

The controller developed in Section IV was specific to a model which was not influenced by the global dynamics of the robotic system, in which case $\theta_\Delta = (q_m)_i - (q)_i$ for $i = 1, \dots, n$. Similarly, the rigid system model in (10) assumed no compliance in the system. The remainder of this section will be devoted to understanding the coupling effects of these previously decoupled systems in the context of RES-CLFs.

Application of RES-CLF Motor Controller. Let $u_d(q, \dot q)$ be a controller that, when applied to the system

$$M(q)\ddot q + H(q, \dot q) = u_d(q, \dot q) \tag{39}$$

drives $y \to 0$. For example, $u_d(q, \dot q)$ can taken to be any controller in $K_\varepsilon(x)$ as developed in Sect. III.

Returning to the SEA model, we can write (38) as

$$J\ddot q_\Delta + b\dot q_\Delta + kq_\Delta = u_m - J\ddot q$$

where $q_\Delta = q_m - q$. Applying the motor controller (33), in its vector form with $\tau_d = u_d(q, \dot q)$, and with J, k, and b replaced by corresponding diagonal matrices with the inertia, damping and spring constant for each motor, yields:

$$\ddot e = \mu - k\ddot q$$

where $e = kq_\Delta - u_d(q, \dot q)$. Writing $z = (e, \dot e)$, we have the following representation of the motor dynamics:

$$\dot z = Fz + G\mu + \begin{bmatrix} 0 \\ -k\ddot q \end{bmatrix}$$

with F and G given as in (34). Motivated by the choice of coordinates in (24), the coordinate transformation $z \mapsto I_\varepsilon z =: z_\varepsilon$ yields the following control system for the motor dynamics:

$$\varepsilon\dot z_\varepsilon = Fz_\varepsilon + G\varepsilon\mu + \varepsilon\begin{bmatrix} 0 \\ -k\ddot q \end{bmatrix}$$

Applying a feedback control law $\mu_\varepsilon(z) \in \overline{K}_\varepsilon(z)$ yields the dynamics:

$$\varepsilon\dot z_\varepsilon = Fz_\varepsilon + G\varepsilon\mu_\varepsilon(z) + \varepsilon\begin{bmatrix} 0 \\ -k\ddot q \end{bmatrix}$$

By (28), this can be equivalently stated as

$$\varepsilon\dot z_\varepsilon = Fz_\varepsilon + G\mu(z_\varepsilon) + \varepsilon\begin{bmatrix} 0 \\ -k\ddot q \end{bmatrix} \tag{40}$$

for $\mu(z_\varepsilon) \in \overline{K}(z_\varepsilon)$. Note that, in this case, the direct mapping between $\overline{K}_\varepsilon(z)$ and $\overline{K}(z_\varepsilon)$ established in Prop. 1 implies that, given $\mu_\varepsilon(z) \in \overline{K}_\varepsilon(z)$, $\mu(z_\varepsilon) = \varepsilon\mu_\varepsilon(I_\varepsilon^{-1}z_\varepsilon)$.

Singular Pertubation Perspective. The dynamics given in (40), coupled with (37), can naturally be viewed as a multitime-scale system. As a result, this system of equations in naturally amendable to singular perturbation theory [10], [11]. In this case, due to the RES-CLF controller applied at

the motor control level, the actuator dynamics of the SEA are viewed as the fast dynamics while the dynamics of the robot are the slow dynamics. The goal is to show that this time-scale separation allows us to approximate (40) and (37) by the rigid model (39).

Lemma 2: *For the system* (40) *evaluated at* $\varepsilon = 0$ *implies that* $z = 0$ *and thus* $kq_\Delta = u_d(q, \dot{q})$. *Therefore, the quasi-steady state system is given by:*

$$M(\bar{q})\ddot{\bar{q}} + H(\bar{q}, \dot{\bar{q}}) \quad = \quad u_d(\bar{q}, \dot{\bar{q}}) \tag{41}$$

with boundary layer system:

$$\frac{d\eta}{d\tau} = F\eta + G\mu(\eta) \tag{42}$$

for $\mu(\eta) \in \overline{K}(\eta)$.

Proof: To show the desired result, it is necessary to establish that $\varepsilon = 0$ implies that $z = 0$. To see this, we begin by evaluating (40) at $\varepsilon = 0$ which implies that $\dot{e} = 0$ and $\mu(z_\varepsilon) = 0$. Since $\mu(z_\varepsilon) \in \overline{K}(z_\varepsilon)$ this implies that

$$z_\varepsilon^T PGG^T P z_\varepsilon \leq 0 \;\Rightarrow\; \|G^T P z_\varepsilon\|^2 = 0 \;\Rightarrow\; G^T P z_\varepsilon = 0.$$

By the CARE (17) this in turn would imply that

$$z_\varepsilon^T (F^T P + PF) z_\varepsilon = -z_\varepsilon^T Q z_\varepsilon$$

which only holds if $z_\varepsilon = 0$ or if F is stable. Since F has eigenvalues on the imaginary axis, i.e., the Lyapunov equation does not have a solution, we therefore have that $z_\varepsilon = 0$. Finally, since $\dot{e} = 0$, multiplying $\varepsilon z_\varepsilon$ is independent of ε, can thus be evaluated at $\varepsilon = 0$, and therefore implies that $e = 0$, or $kq_\Delta = u_d(q, \dot{q})$. Thus (41) is established. Finally, (42) follows from (40) with the change of variables $\eta = z_\varepsilon$ together with the quasi-steady state conditions. ■

Therefore, we have established that the quasi-steady state dynamics of the system are just the rigid body dynamics (39) for which u_d was originally designed to stabilize.

Main result. Utilizing the result of singular pertubation analysis applied to the SEA model, we can now establish the main result of this paper. In particular, we will show that the choice of embedded level controller implies that, for ε sufficiently small, the dynamics of the SEA model can be approximated by the rigid model.

Theorem 1: *Consider the model of a SEA system given in* (37) *and* (38). *For*

$$u_d(q, \dot{q}) = A(q, \dot{q})^{-1}(-L_f^2(q, \dot{q}) + \mu_\varepsilon(x)) \tag{43}$$

$$u_m(z, u_d(q, \dot{q})) = \frac{J}{k}\mu_\varepsilon(z) + \begin{bmatrix} 1 & \frac{b}{k} \end{bmatrix} z + u_d(q, \dot{q}) \tag{44}$$

with $\mu_\varepsilon(x) \in K_\varepsilon(x)$ *twice differentiable and* $\mu_\varepsilon(z) \in \overline{K}_\varepsilon(z)$ *Lipschitz continuous, it follows that there exists an* $\varepsilon^* > 0$ *such that*

$$\left\| \begin{array}{c} y(t) \\ \dot{y}(t) \end{array} \right\| \leq \frac{1}{\varepsilon}\sqrt{\frac{\lambda_{\max}(P)}{\lambda_{\min}(P)}} e^{-\frac{1}{\varepsilon}\frac{\lambda_{\min}(Q)}{2\lambda_{\max}(P)}t} \left\| \begin{array}{c} y(0) \\ \dot{y}(0) \end{array} \right\| + O(\varepsilon)$$

for all $0 \leq \varepsilon \leq \varepsilon^*$ *and* P *satisfying* (17).

Proof: This result follows from the application of Tikhonov's theorem [10], [11] coupled with Lemma 1 and Lemma 2. ■

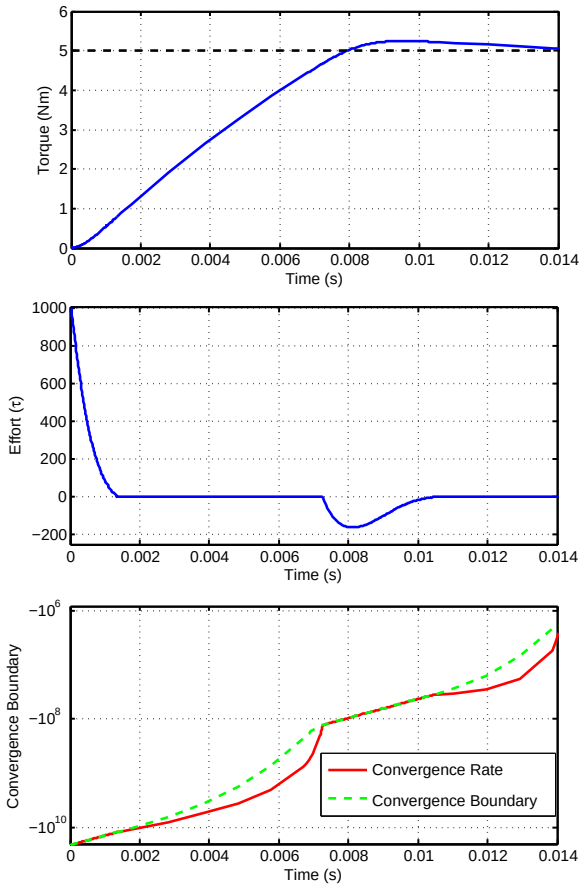

Fig. 2. The step response of the controller is optimal and meets the convergence constraints. The output of the controller is nonsmooth and zero when the dynamics of the system are already converging and require no control effort. The convergence rate of this simulation is $\frac{1}{\varepsilon} = 1100$.

VI. Results: Simulation and Experimental

We conclude the paper with simulation and experimental results demonstrating the performance of the quadratic program based embedded controller. Importantly, we are able to demonstrate through hardware tests (see Fig. 1 and the corresponding video at [1]) that the proposed controller is able to accurately track a variety of torque signals, even in the presence of unknown disturbances.

Implementation. From a practical implementation perspective, it is useful to have a simple closed form expression for the control law (36); this will allow the controller to run in real-time at an embedded control level. Because of the simple form of F_m and G_m in (34), it can be verified that the solution to the CARE (17), with $Q = I$, is given by:

$$P = \begin{bmatrix} \sqrt{3} & 1 \\ 1 & \sqrt{3} \end{bmatrix}, \quad \Rightarrow \quad P_\varepsilon = \begin{bmatrix} \frac{1}{\varepsilon^2}\sqrt{3} & \frac{1}{\varepsilon} \\ \frac{1}{\varepsilon} & \sqrt{3} \end{bmatrix} \tag{45}$$

This allows for the direct calculation of V_ε as:

$$V_\varepsilon(\theta_\Delta, \dot{\theta}_\Delta, \tau_d) = \tag{46}$$
$$\sqrt{3}\frac{1}{\varepsilon^2}\left(\tau_d - k\theta_\Delta\right)^2 + 2\frac{1}{\varepsilon}k\left(-\tau_d + k\theta_\Delta\right)\dot{\theta}_\Delta + \sqrt{3}k^2\dot{\theta}_\Delta^2$$

With these constructions, it is easy to explicitly calculate $L_{F_m}V_\varepsilon$ and $L_{G_m}V_\varepsilon$ in (19). This allows for the direct calculation of $\psi_{0,\varepsilon}$ and $\psi_{1,\varepsilon}$ in (8) with γ given in (45) and V_ε given in (46), which in turn allows for the final closed form expression of $\overline{\psi}_{0,\varepsilon}$ and $\overline{\psi}_{1,\varepsilon}$ as given in (35). This yields the final form of the controller as given in (36).

It is important to note that in (46), the desired torque is viewed as a constant. This simplification was chosen for initial implementation to observe exponential convergence of the step response. In order to track more complex desired signals, the derivative of desired torque would necessarily be added to the controller; the ability of the torque controller to achieve accurate tracking of signals and disturbances in the experiments can be attributed to the fast control loop rate of the embedded system.

Simulation Results. The controller (36), representing the closed form solution of (Motor QP), was implemented in simulation and a step response was conducted to observe the behavior of the controller. Data regarding output torque, motor torque effort (τ_m) and the convergence conditions used in the min-norm controller were collected to demonstrate the effects of a nonlinear control system achieving its control objective on a modeled series elastic actuator.

By simulating a step response, the nonlinearity of the controller can be observed. In Fig. 2 it can be noted that the slope of the torque is smooth and converges on on the control objective, i.e., the desired torque. The motor control effort is nonsmooth and has several intervals where no control effort is exerted. These intervals correspond with areas where the natural dynamics of the system achieve the desired convergence of V_ε, i.e., intervals where $\dot{V}_\varepsilon \leq -\frac{1}{\varepsilon}\gamma V_\varepsilon$ without the need to exert control effort. Thus, the controller utilizes the natural dynamics of the system to realize the control objective.

Experimental Results. The controller was tested experimentally on a SEA through the setup shown in Fig. 1; in particular, it was implemented on an embedded motor driver at a control rate of 5kHz, necessarily using the closed form solution of the QP. Because the implementation of the controller in hardware is subject to additional constraints, the simulation was altered by adding saturation after the QP calculated its requested effort. This directly corresponds to current limits, and therefore motor torque limits, that exist on the motor driver hardware used in the experiments.

For the first set of tests, the series elastic actuator output was fixed, which allows easier system identification and modeling of the parameters that are used in the closed form representation of the QP. With the output fixed, a step response for several different values of ε was measured and can be seen in Fig. 3 with the modified simulation results. The output of the controller, τ_m was also measured at the embedded level by collecting motor current data. Smooth convergence to the control objective can be seen in Fig. 3. More importantly, this coincides with periods where the measured output of the motor controller is zero, confirming the nonsmooth embedded controller is behaving at the embedded

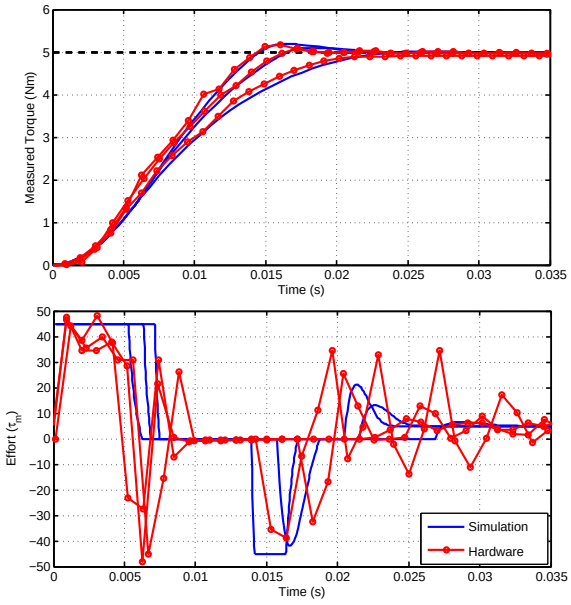

Fig. 3. Experimental step response with $\frac{1}{\varepsilon}$ = 1100, 900, and 700. Simulation (blue) is set to saturate at the approximate value based upon observed hardware limits and compared against experimental data (red). The hardware exhibits the same behavior as simulation, i.e., it does not exert control effort when the system dynamics meet the convergence constraint (CLF Constraint).

level similarly to the simulation—according to (Motor QP), no control effort will be exerted if the convergence rate is satisfied passively. This demonstrates the torque optimal nature of the RES-CLF based QP controller.

For robotic systems, it is also important for an actuator to track nontrivial torque trajectories. To understand the performance of the controller, sine, chirp, and square wave signals were provided to the embedded controller. Fig. 4 shows the torque controller was able to accurately and consistently track its objective with minimal error on different time scales.

To further characterize the performance of the controller, the actuator was freed and a 10lbs weight was attached to the joint output via a 1ft link (this setup is demonstrated in the left picture in Fig. 1). The dynamics of the weight at the output were unmodeled and therefore can be treated as a disturbance; this tests the robustness of the controller in achieving its objective without the need for additional modeling and/or calculations that cannot be performed at the embedded level. The top plot of Fig. 5 shows that torque tracking of a sine wave in this scenario—the results indicate that minimal tracking error is achieved.

The ability of the controller to reject unknown joint disturbances is also necessary for implementation in a robotic system operating in uncertain environments. The middle and bottom plots of Fig. 5 show the ability for the controller to track a torque trajectory and a steady state torque while a human actively perturbed the output link of the actuator. The controller exhibited error of less than 0.2 Nm throughout operation, more often reducing tracking error to below 0.1 Nm despite active disturbances to the output. A video

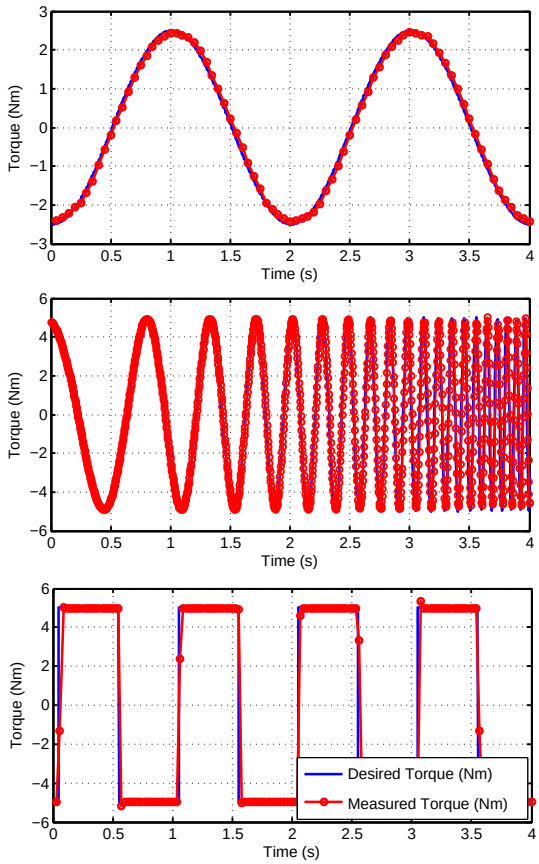

Fig. 4. Torque tracking of nontrivial signals yields only small amounts of error. Chirp signals were tested through 20 Hz with no deterioration of torque tracking ability. This set of experiments was conducted while the actuators output was locked. For all plots, $\frac{1}{\varepsilon} = 900$.

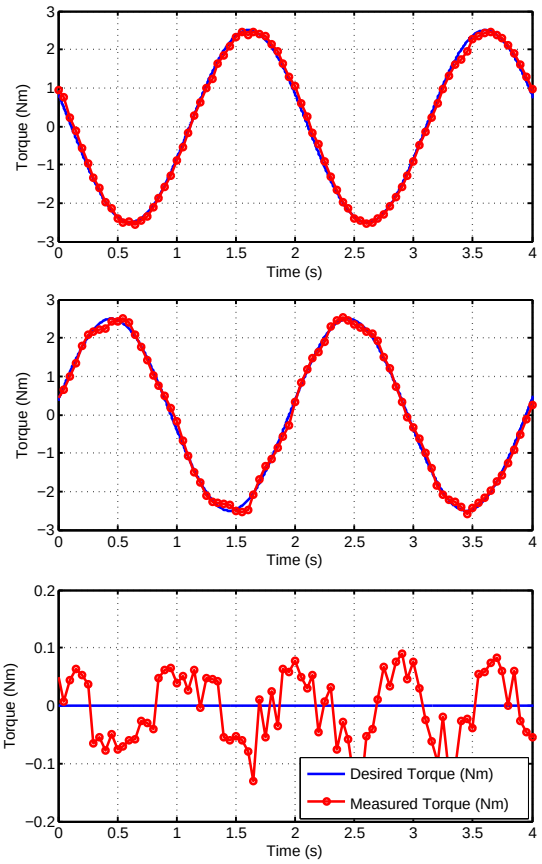

Fig. 5. The controller exhibits good disturbance rejection. The top plot is the actuators ability to track torque with a moving, unknown output load. The bottom two plots show torque tracking for sine waves and steady state with human-interaction with the system. For all plots, $\frac{1}{\varepsilon} = 900$.

demonstrating the ability of QP based embedded controller to simultaneously reject unmodeled dynamics (a 10lbs weight positioned 1ft from the joint) and human-interaction can be found at [1].

References

[1] Hardware demonstration of RES-CLF based QP on a series elastic actuator. http://youtu.be/rCyyjuDs1BQ.

[2] A. D. Ames, K. Galloway, and J. W. Grizzle. Control Lyapunov Functions and Hybrid Zero Dynamics. *Proc. 51st IEEE Conf. Decision and Control*, 2012.

[3] A. D. Ames, K. Galloway, J. W. Grizzle, and K. Sreenath. Rapidly Exponentially Stabilizing Control Lyapunov Functions and Hybrid Zero Dynamics. *To appear in IEEE Trans. Automatic Control*, 2014.

[4] A. D. Ames and M. Powell. Towards the unification of locomotion and manipulation through control lyapunov functions and quadratic programs. In *Control of Cyber-Physical Systems, Lecture Notes in Control and Information Sciences*, volume 449, pages 219–240, 2013.

[5] Zvi Artstein. Stabilization with relaxed controls. *Nonlinear Analysis: Theory, Methods & Applications*, 7(11):1163–1173, 1983.

[6] R. A. Freeman and P. V. Kokotović. *Robust Nonlinear Control Design*. Birkhäuser, 1996.

[7] K. Galloway, K. Sreenath, A. Ames, and J. Grizzle. Walking with Control Lyapunov Functions (2012). Youtube Video. [Online]. Available: http://youtu.be/onOd7xWbGAk.

[8] K. Galloway, K. Sreenath, A. D. Ames, and J.W. Grizzle. Torque saturation in bipedal robotic walking through control lyapunov function based quadratic programs. Technical report, 2013.

[9] J.W. Hurst, J.E. Chestnutt, and A.A. Rizzi. The actuator with mechanically adjustable series compliance. *Robotics, IEEE Transactions on*, 26(4):597–606, 2010.

[10] H.K. Khalil. *Nonlinear Systems - 3rd Edition*. Prentice Hall, Upper Saddle River, NJ, 2002.

[11] P. Kokotovic, H. K. Khalil, and J. O'Reilly. *Singular Perturbation Methods in Control: Analysis and Design*. Academic Press, 1986.

[12] B. Morris and J.W. Grizzle. Hybrid invariance in bipedal robots with series compliant actuators. In *Decision and Control, 2006 45th IEEE Conference on*, pages 4793–4800, 2006.

[13] N. Paine, S. Oh, and L. Sentis. Design and control considerations for high-performance series elastic actuators. To appear in IEEE/ASME Transactions on Mechatronics, 2014.

[14] G.A. Pratt and M.M. Williamson. Series elastic actuators. In *Intelligent Robots and Systems 95. 'Human Robot Interaction and Cooperative Robots', Proceedings. 1995 IEEE/RSJ International Conference on*, volume 1, pages 399–406 vol.1, 1995.

[15] Jerry E. Pratt and Benjamin T. Krupp. Series elastic actuators for legged robots, 2004.

[16] S. Sastry. *Nonlinear Systems: Analysis, Stability and Control*. Springer Verlag, 1999.

[17] E. Sontag. A Lyapunov-like stabilization of asymptotic controllability. *SIAM Journal of Control and Optimization*, 21(3):462–471, 1983.

[18] E. Sontag. A 'universal' contruction of Artstein's theorem on nonlinear stabilization. *Systems & Control Letters*, 13:117–123, 1989.

[19] Mark W. Spong. Adaptive control of flexible joint manipulators. *Systems & Control Letters*, 13(1):15 – 21, 1989.

[20] K. Sreenath, H-W. Park, I. Poulakakis, and J.W. Grizzle. Embedding active force control within the compliant hybrid zero dynamics to achieve stable, fast running on mabel. *International Journal of Robotics Research*, 32(1):324–345, 2013.